ISSN: 1410-8917
Jurnal Kimia Sains & Aplikasi
e-ISSN: 2597-9914

Jurnal Kimia Sains dan Aplikasi 29 (6) (2026): 396-404

Jurnal Kimia Sains dan Aplikasi
Journal of Scientific and Applied Chemistry

Journal homepage: http://ejournal.undip.ac.id/index.php/ksa

Synthesis of Activated Carbon/Magnetite Nanocomposite Modified with Povidone for Adsorption Applications of Heavy Metal Ions

Muhammad Zainullah [1], Muhammad Safwan Aziz [2], Nurul Hidayat [1], Lya Rizka Herawati [1], Ahmad Taufiq [1,*]

[1] Department of Physics, Faculty of Mathematics and Natural Sciences, Universitas Negeri Malang, Malang 65145, Indonesia
[2] Laser Center, Ibnu Sina Institute for Scientific and Industrial Research, Universiti Teknologi Malaysia, 81310 Skudai, Malaysia

* Corresponding author: ahmad.taufiq.fmipa@um.ac.id

https://doi.org/10.14710/jksa.29.6.396-404

Article Info

Article history:

Received: 11th April 2026
Revised: 11th June 2026
Accepted: 18th June 2026
Online: 31st July 2026

Keywords:
Activated carbon/magnetite; Povidone modification; Lead heavy metal; Adsorption; Wastewater

Abstract

This study reports on activated carbon/magnetite nanocomposite modified with povidone for the adsorption applications of heavy metal (lead) ions. The synthesis routes used in this study were coprecipitation, activated carbon activation, and ex-situ methods. The data analysis results showed that the activated carbon/magnetite nanocomposite modified with povidone had a crystallite size of 9.45 nm with a single-phase inverse cubic spinel structure. The activated carbon/magnetite nanocomposite modified with povidone showed successful synthesis with the appearance of octahedral and tetrahedral Fe–O lattice vibrations (440 and 550 cm^{-1}), O–H (3200–3395 cm^{-1}), C=O (1655 cm^{-1}), and C– N (1182 cm^{-1}) functional groups. Furthermore, the activated carbon/magnetite nanocomposite modified with povidone exhibited a chunky and spherical morphology, with a particle size of 39.91 nm. The nanocomposite had a large specific surface area and pore volume, namely 129.237 m^2/g and 0.198 cm^3/g, respectively, thus providing many active sites for adsorption. Interestingly, the nanocomposite was superparamagnetic, facilitating its separation from the solution after adsorption. The adsorption efficiency of this nanocomposite was 71.01% with an adsorption capacity of 29.6415 mg/g in 180 minutes at a volume of heavy metal solution of 25 mL with a theoretical concentration of 100 ppm, adsorbent dose of 0.05 g, pH 5, and room temperature, and followed with pseudo-second order adsorption kinetics model. The resulting removal efficiency is better than magnetite/povidone, which has a removal efficiency of 70%.

1. Introduction

Wastewater generated from various industrial activities, including battery manufacturing, automobile production, electroplating, electronics, paint, steel, ceramics, dye, and fertilizer industries, is a major source of lead contamination in aquatic environments [1, 2]. Lead is one of the most hazardous heavy metals due to its non-biodegradable nature, persistence in the environment, and tendency to bioaccumulate throughout the food chain, resulting in severe toxic effects on living organisms [3, 4]. Human exposure to lead has been associated with numerous adverse health effects, including abdominal pain, neurological impairment, kidney dysfunction, cardiovascular disease, respiratory disorders, and, in severe cases, death [5, 6]. According to the World Health Organization (WHO), lead exposure was responsible for more than 1.5 million deaths and approximately 33 million disability-adjusted life years (DALYs) worldwide in 2021 [6]. Furthermore, lead concentrations in many Indonesian water bodies have been reported to exceed the WHO permissible limit for drinking water of 0.01 mg/L [7]. Therefore, the development of effective technologies for removing lead from contaminated wastewater is of critical importance.

Various technologies have been developed for the removal of lead from industrial wastewater, including ion exchange, liquid membrane separation, membrane filtration, electrocoagulation, chemical precipitation, and adsorption [8, 9]. However, many of these techniques suffer from inherent limitations, such as secondary waste generation, membrane fouling or operational instability, high chemical and energy consumption, and the strong dependence of ion-exchange performance on resin properties and solution chemistry [8, 10]. Among these technologies, adsorption is considered one of the most promising approaches because of its high removal efficiency, low operating cost, operational simplicity, and the potential for adsorbent regeneration and reuse [11, 12].

In adsorption applications, magnetite has received considerable attention owing to its excellent magnetic properties, low toxicity, and environmental compatibility [13]. Its superparamagnetic behavior enables rapid separation from aqueous solutions using an external magnetic field, facilitating adsorbent recovery while minimizing material loss and the generation of secondary pollution [14, 15]. Despite its advantages, magnetite still faces challenges: it is easily oxidized when exposed to air or acids, thereby reducing its magnetic properties. Furthermore, magnetite easily agglomerates, reducing its dispersibility [16, 17].

To overcome the oxidation and agglomeration of magnetite, surface modification with povidone (polyvinylpyrrolidone, PVP) has been widely employed. Povidone forms a protective coating on the magnetite surface through coordination between its carbonyl groups and surface Fe ions, providing steric stabilization that suppresses particle aggregation and limits crystal growth. Consequently, the modified particles exhibit improved oxidation resistance, enhanced dispersion stability, and more uniform crystal sizes [18].

Previous studies have demonstrated that povidone modification reduced the average particle size of magnetite from 857 nm to 225 nm and produced smaller, more homogeneous crystals [18]. In addition, magnetite/povidone adsorbents have been reported to achieve approximately 70% removal efficiency for Cu(II) ions [19]. Although these findings demonstrate the potential of povidone-modified magnetite, its adsorption performance remains limited, possibly due to its relatively low specific surface area. To address this limitation, incorporating activated carbon is a promising strategy owing to its high porosity, large specific surface area, and abundant surface functional groups that provide additional adsorption sites for heavy metal ions [20, 21]. Therefore, this study developed a povidone-modified activated carbon/magnetite nanocomposite as an adsorbent for removing Pb(II) ions from aqueous solutions.

2. Experimental

2.1. Materials

The materials used in this study included dry iron sand, dried old coconut shells, Povidone K–30, hydrochloric acid (HCl, 2 M), ammonium hydroxide (NH_4OH, 6.5 M), nitric acid (HNO_3, 2 M), distilled water, deionized water, methanol, 70% ethanol, and lead nitrate ($Pb(NO_3)_2$) as the Pb(II) source.

2.2. Experimental

Cleaned and ground coconut shell charcoal was first carbonized at 600°C in a non-inert atmosphere (air) using a muffle furnace to remove volatile components. The resulting charcoal was then chemically activated by soaking in 2 M HNO_3 for 2 h, followed by washing with 70% ethanol until neutral and drying in an oven to obtain activated carbon powder [22]. Meanwhile, 20 g of separated iron sand was dissolved in 58 mL of 2 M HCl to produce $FeCl_2$ and $FeCl_3$ in a theoretical Fe^{2+}/Fe^{3+} molar ratio of 1:2 based on the stoichiometric dissolution of magnetite, as described by Equation (1).

$$Fe_3O_4 + 8HCl \rightarrow FeCl_2 + 2FeCl_3 + 4H_2O \quad (1)$$

A 1.5% (w/v) Povidone K–30 solution was added to the $FeCl_2/FeCl_3$ solution, after which NH_4OH (6.5 M) was added dropwise until precipitation occurred. No additional oxidation or reduction treatment was applied during the dissolution process. The resulting precipitate was washed repeatedly with methanol and distilled water until a neutral pH was achieved, and then dried in an oven to obtain povidone-modified magnetite powder [23].

The activated carbon and povidone-modified magnetite were separately dispersed in deionized water, mixed, and sonicated until a homogeneous suspension was obtained. The suspension was subsequently dried in an oven to produce the activated carbon/magnetite nanocomposite modified with povidone, with a final product yield of approximately 90% [24].

Batch adsorption experiments were performed by mixing 0.05 g of adsorbent with 25 mL of a 100 ppm Pb(II) solution under continuous stirring at 720 rpm. After adsorption, the adsorbent was separated magnetically, sieved, and the residual Pb(II) concentration in the filtrate was analyzed. The adsorption capacity (q_e) and Pb(II) removal efficiency were calculated using Equations (2) and (3), respectively [25].

$$q_e = \frac{C_0 - C_e}{m} \times V \quad (2)$$

$$\%Removal = \frac{C_0 - C_e}{C_0} \times 100\% \quad (3)$$

2.3. Characterization

The synthesized materials were characterized using several analytical techniques. X-ray diffraction (XRD; X'Pert PRO) was employed to determine the crystal structure and crystallite size. The crystallite size was estimated by Rietveld refinement using Rietica software. Surface morphology and elemental composition were analyzed using scanning electron microscopy coupled with energy-dispersive X-ray spectroscopy (SEM–EDX; FEI Inspect S50). Functional groups were identified using Fourier transform infrared spectroscopy (FTIR; Shimadzu IRPrestige-21). Magnetic properties were evaluated using a vibrating sample magnetometer (VSM; Quantum Design PPMS® VersaLab™ Cryogen-Free 3 Tesla). The specific surface area, pore volume, and average pore diameter were determined using the Brunauer–Emmett–Teller (BET) method with a Micromeritics TriStar II Plus 3020 analyzer (P/N 302/00000/22). The adsorption performance toward

Pb(II) ions was evaluated by measuring the residual lead concentration using atomic absorption spectroscopy (AAS; Thermo Scientific iCE 3000).

3. Results and Discussion

The XRD pattern of the activated carbon/magnetite nanocomposite modified with povidone exhibits the characteristic inverse cubic spinel structure of magnetite, consistent with AMCSD model No. 0007423, as shown in Figure 1. The most intense diffraction peak appears at 2θ = 35.59°, corresponding to the (311) crystal plane. Additional diffraction peaks are observed at 2θ = 30.20°, 43.33°, 53.76°, 57.30°, and 62.90°, which are indexed to the (220), (400), (422), (511), and (440) crystal planes, respectively. These diffraction peaks agree well with those reported for magnetite in previous studies [26]. The addition of povidone does not change the magnetite diffraction pattern [27]. The absence of activated carbon peaks is due to its amorphous nature; these results are consistent with previously reported studies [28, 29].

The results of quantitative analysis indicate that the size of magnetite crystallites is 9.45 nm, with a lattice parameter of 8.350 Å. This crystallite size is considerably smaller than the previously reported value of 17.69 nm for unmodified magnetite [30], suggesting that povidone effectively suppresses crystal growth during nanoparticle formation. The polymer likely acts as a capping or stabilizing agent, limiting crystal growth while promoting nucleation, thereby producing smaller crystallites [31]. The measured lattice parameter is slightly lower than the standard value for bulk magnetite (approximately 8.39–8.40 Å). This slight contraction may be attributed to nanoscale size effects and an increased density of lattice defects, both of which can influence the crystal lattice parameters [32].

The FTIR results are shown in Figure 2 and Table 1. The strong peaks at 3200–3395 cm^{-1} can be attributed to the stretching vibrations of the hydroxyl (OH) groups in alcohols and phenols, which are part of organic bonds. These results are consistent with previous research reports, which assign functional groups at wavenumbers between 3200–3645 cm^{-1} to O–H bond vibrations [33]. At wavenumbers of 440 cm^{-1} and 550 cm^{-1}, Fe–O lattice vibrations associated with tetrahedral and octahedral sites in the spinel structure of magnetite were identified, respectively [34]. Meanwhile, the aromatic C–H ring group and the out–of–plane bend aromatic C–H in activated carbon are detected at wavenumbers of 814 cm^{-1} and 881 cm^{-1}, respectively [35, 36].

The stretching of single C–O bonds in activated carbon is formed at wavenumbers of 918–1146 cm^{-1} [36, 37]. In addition, aromatic activated carbon compounds contain a C=C double bond at a wavenumber of 1607 cm^{-1} [35]. The C–N stretching band of povidone is located at a wave number of 1182 cm^{-1} [38]. Meanwhile, other identified povidone functional groups are –C=O primary amide stretching and asymmetric CH_2 stretching at a wavenumber of 1655 cm^{-1}, respectively. Furthermore, there are vibrations at 2839 and 2878 cm^{-1} which are associated with the C–H stretching mode in povidone [39].

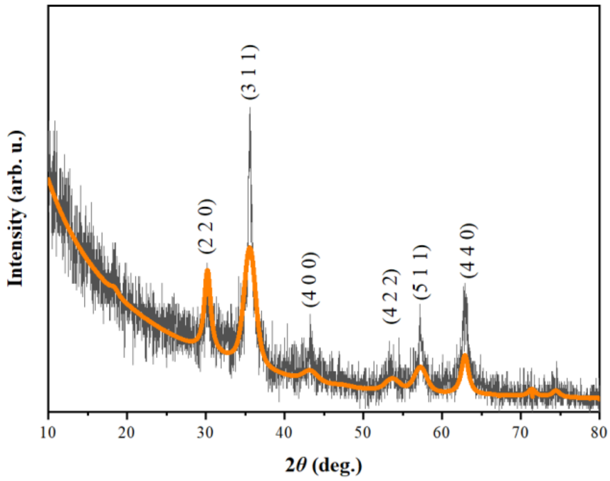

Figure 1. XRD pattern of activated carbon/magnetite nanocomposite modified with povidone

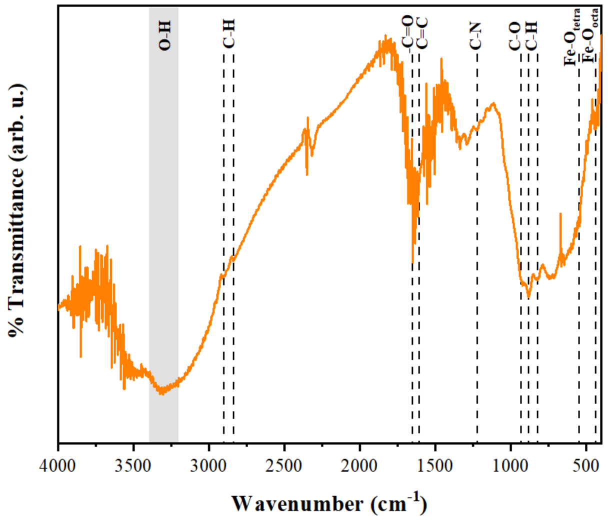

Figure 2. FTIR spectrum of activated carbon/magnetite nanocomposite modified with povidone

Table 1. FTIR results of activated carbon/magnetite nanocomposite modified with povidone

Peak position (cm^{-1})	Assignment	Component
440	Fe–O octahedral	Fe_3O_4
550	Fe–O tetrahedral	Fe_3O_4
814	Aromatic ring C-H	Activated carbon
881	Aromatic C-H out-of-plane bend	Activated carbon
918–1146	stretching of single C–O bonds	Activated carbon
1182	C–N stretching	PVP
1607	C=C double bond	Activated carbon
1655	–C=O stretching	PVP
2839	C–H stretching	PVP
2878	C–H stretching	PVP
3200–3395	O–H bond	Activated carbon

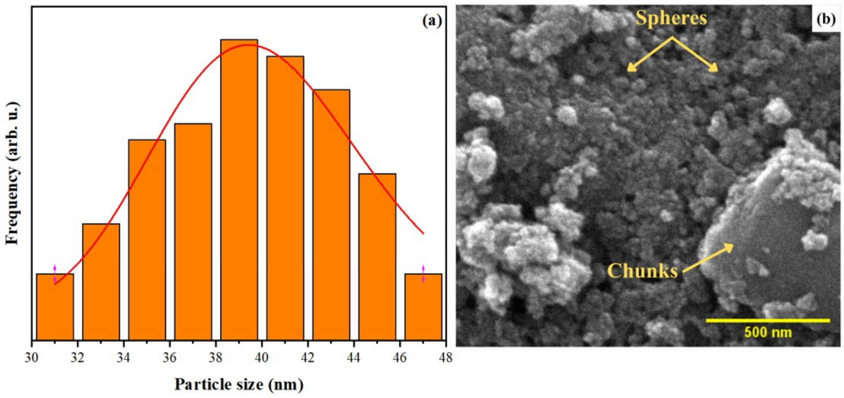

Figure 3. (a) Particle size and (b) morphology of activated carbon/magnetite modified with povidone

Figure 3(a) shows the surface morphology of activated carbon/magnetite nanocomposite modified with povidone from SEM image results, where this nanocomposite has a morphology in the form of chunks (asymmetric or irregular) of activated carbon and spheres of magnetite modified with povidone. The analysis result in Figure 3(b) shows that the size of spherical magnetite particles is 39.91 nm. In previous research, the size of magnetite particles was 63.19 nm [30]. This result indicates that povidone successfully forms a protective layer on magnetite, thereby reducing agglomeration and particle size [18].

There is a discrepancy between the sizes obtained from the XRD and SEM results. This difference is caused by the size obtained from XRD (9.45 nm) representing the size of a single crystallite from a coherent diffraction domain, while the particle size measured from SEM (39.91 nm) corresponds to the physical dimensions of the particles, which may consist of several crystallites and agglomerated structures [40]. The EDX result shows carbon (C) as the most abundant element at 52.36%. This is due to the high composition of activated carbon. Meanwhile, the oxygen (O) composition is 28.14%, and iron (Fe) is 18.14%. Apart from that, there are impurities in the form of silicon (Si) and titanium (Ti), which most likely originate from the natural precursor material, magnetite, namely iron sand.

The results of the VSM characterization are in the form of a hysteresis loop curve of the activated carbon/magnetite nanocomposite modified with povidone, as shown in Figure 4. The analysis results show that the nanocomposite has a saturation magnetization (M_s) value of 14.64 emu/g. Meanwhile, the remanent magnetization (M_r), coercivity field (H_c), and susceptibility (χ) values are 0.01 emu/g, 23.32 Oe, and 6.87 $\times 10^{-5}$, respectively. Based on the results of this analysis, it can be seen that the nanocomposite exhibits near-superparamagnetic/soft magnetic properties with negligible remanence as indicated by an S-shaped curve, a high M_s value with a small magnetic field, a M_r value close to 0 emu/g, and a low H_c [41].

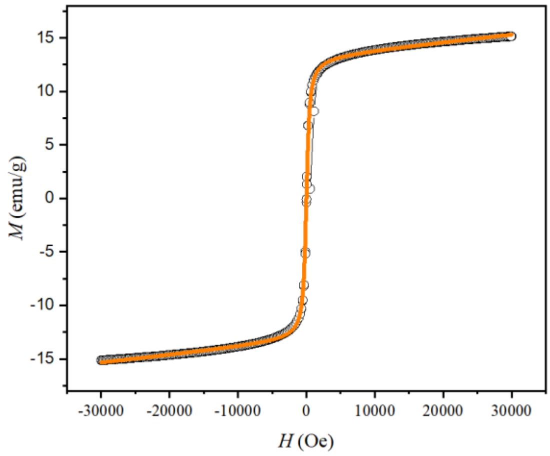

Figure 4. Hysteresis curve of activated carbon/magnetite nanocomposite modified with povidone

The pore structure of activated carbon/magnetite nanocomposites modified with povidone was characterized using BET with N_2 adsorption. It can be seen from Figure 5(a) that the N_2 adsorption–desorption isotherm of activated carbon/magnetite modified with povidone indicates that the material is mesoporous. Mesoporous materials are characterized by having a typical type IV shape curve, and in the range of P/P_0 = 0.2–0.9, a clear H3 hysteresis loop is formed. This H3 hysteresis loop is generally caused by the accumulation of sheet-shaped particles that form slit pores [42]. Referring to the pore size classification according to IUPAC, Figure 5(a) shows that activated carbon/magnetite modified with povidone is mostly mesoporous (2–50 nm) [43]. Furthermore, the measured volume of the nanocomposite is 0.19 cm^3/g. Meanwhile, the nanocomposite has a specific surface area of 129.24 m^2/g as measured by BET and a pore diameter of 5.78 nm, as shown in Figure 5(b). This nanocomposite has a high specific surface area, large pore volume, and small pore diameter. The attachment of povidone-modified magnetite to the surface of activated carbon causes blockage of the macropores, which leads to the loss of macropores in the composite material [44].

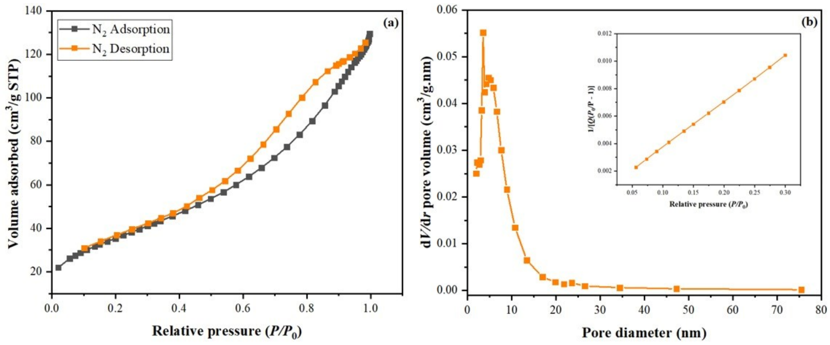

Figure 5. (a) N_2 adsorption–desorption isotherm plot and (b) surface area and pore size distribution of activated carbon/magnetite nanocomposite modified with povidone

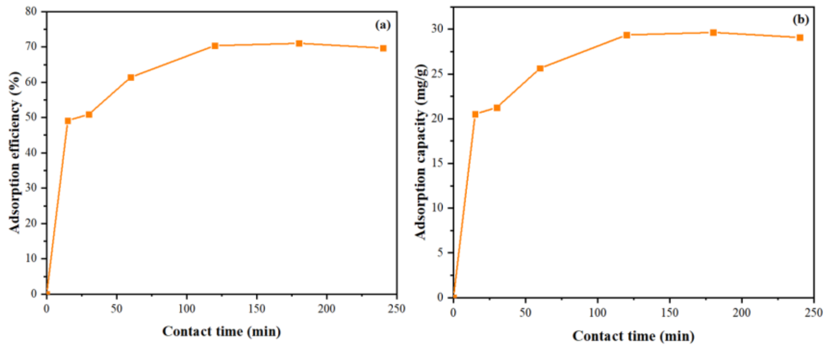

Figure 6. Effect of contact time on (a) removal efficiency and (b) adsorption capacity of the activated carbon/magnetite nanocomposite modified with povidone

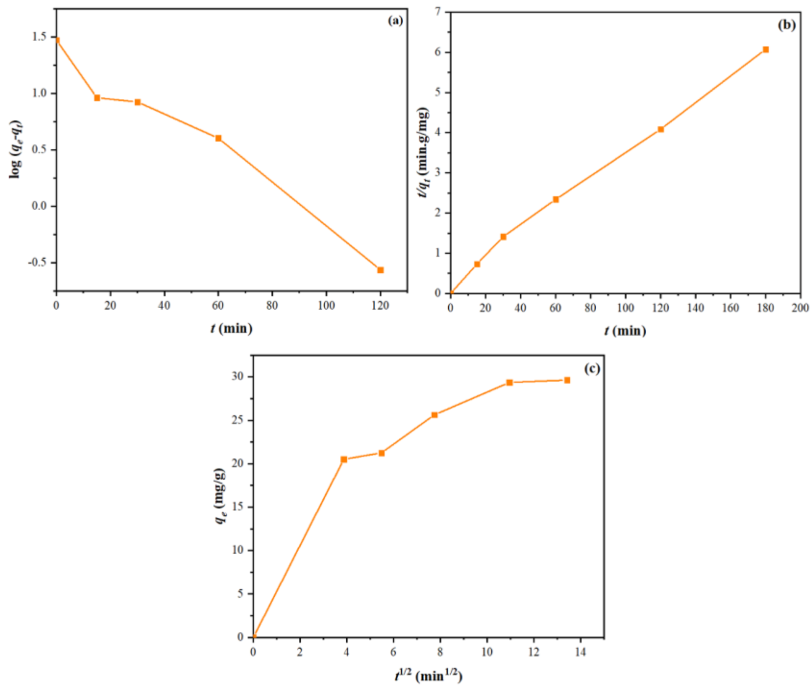

Figure 7. Graph of adsorption kinetics modeling of activated carbon/magnetite nanocomposite modified with povidone (a) Pseudo-first-order, (b) Pseudo-second-order, and (c) Intra-particle diffusion

Figures 6(a) and 6(b) illustrate the removal efficiency and adsorption capacity of the activated carbon/magnetite nanocomposite modified with povidone at different contact times. The adsorption experiments were performed at pH 5, using 25 mL of a 100 ppm heavy-metal solution, an adsorbent dosage of 0.05 g, and at room temperature. The adsorption equilibrium was reached after 180 minutes, corresponding to a removal efficiency of 71.01% and an adsorption capacity of 29.64 mg/g.

The adsorption capacity increased rapidly during the first 15 minutes and then gradually approached equilibrium at 30, 60, 120, and 180 minutes. The rapid initial adsorption is attributed to the abundance of available active sites on the adsorbent surface, allowing efficient adsorption through surface interactions, electrostatic attraction, and ion exchange. As the contact time increased, the number of available adsorption sites gradually decreased, resulting in a slower adsorption rate until equilibrium was attained. A slight decrease in adsorption capacity was observed at 240 minutes, which may be attributed to desorption, re-equilibration of the adsorption system, or experimental variability [11].

The analysis of the adsorption kinetic model is shown in Table 2 and Figures 7(a)–(c). Based on the analysis results, the adsorption of lead by activated carbon/magnetite nanocomposites modified with povidone is consistent with the pseudo-second-order kinetic model, with a correlation coefficient (R^2) of 0.9953. The maximum adsorption capacity (q_e) value obtained with the pseudo-second-order model is 30.6748 mg/g, where this value is close to the experimental adsorption value of 29.6415 mg/g. These results also show that the pseudo-first-order and intra-particle diffusion models are less suitable.

In general, an activated carbon/magnetite nanocomposite modified with povidone for lead adsorption in water has an experimental adsorption capacity of up to 29.6415 mg/g. This result is better compared to other adsorbents that have been used in previous studies, such as $Fe_3O_4@SiO_2$–TMPDT, which has a lead adsorption capacity of 11.760 mg/g [45] and polyamide thin–film composite/polyethersulfone–coreshell–Fe_3O_4/ZnO, which has a lead adsorption capacity of 8.8573 mg/g [46]. Activated carbon/magnetite nanocomposites modified with povidone are superior because activated carbon-based materials show better adsorption because adsorption capacity depends strongly on operating conditions; comparisons are indicative rather than absolute unless tested under identical conditions.

Table 2. Kinetic model parameters for the adsorption of heavy metal ions onto the activated carbon/magnetite nanocomposite modified with povidone

Kinetic model	Parameter	Value
Pseudo-first-order	q_e (mg/g)	24.5188
	k_1 (min^{-1})	0.0158
	R^2	0.9685
Pseudo-second-order	q_e (mg/g)	30.6748
	k_2 (g.mg/min)	0.0044
	R^2	0.9953
Intra–particle diffusion	C (mg/g)	7.0521
	k_i (mg/g.min$^{-½}$)	2.0282
	R^2	0.8018
Experimental	q_e (mg/g)	29.6415

4. Conclusion

Activated carbon/magnetite nanocomposite modified with povidone was successfully synthesized with an inverse cubic spinel crystal structure and a particle size of 9.45 nm. This nanocomposite has several active groups, such as O–H, C=O, and C–N, that play a role in the adsorption process. The nanocomposite also has unique characteristics with a small particle size, resulting in a large specific surface area that can increase the adsorption capacity. The nanocomposite also has strong magnetic properties that facilitate separation after adsorption. The nanocomposite has an adsorption efficiency of 71.01% and an adsorption capacity of 29.6415 mg/g in 180 minutes. The adsorption kinetics best fit a pseudo-second-order model. Thus, the application of activated carbon/magnetite nanocomposite modified with povidone in water purification can be a promising low-complexity adsorbent candidate with magnetic recoverability for removing lead in wastewater. For further research development, cost and regeneration/reuse analysis can be carried out for adsorbent feasibility analysis before use in industrial wastewater treatment processes.

Acknowledgement

This research is funded by the Kementerian Pendidikan Tinggi, Sains, dan Teknologi through the PPS-PTM scheme under contract number 2.6.154/UN32.14.1/LT/2025.

References

[1] Madeeha Younes, Muhammad Younas, Sidra Shaoor Kiani, Amjad Farooq, Saima Ashraf, Rimsha Shoukat, Zainab Waseem, Muhammad Zayed, Single and Dual Metal Impregnated Activated Carbons for the Removal of Lead and Chromium from Wastewater, *Journal of Water Chemistry and Technology*, 48, (2026), 12-26 https://doi.org/10.3103/S1063455X26010078

[2] Cléophée Gourmand, Caroline Bertagnolli, Bénédicte Prelot, Anne Boos, Véronique Hubscher-Bruder, Jérémy Brandel, Competitive adsorption mechanisms of Cd(ii), Cu(ii) and Pb(ii) on bioinspired mesoporous silica revealed by complementary adsorption/isothermal titration calorimetry studies, *Dalton Transactions*, 53, 8, (2024), 3690-3701 https://doi.org/10.1039/D3DT03210H

[3] Hassan Majiya, Francis Clegg, Chris Sammon, Bentonite-Chitosan Composites or Beads for Lead (Pb) Adsorption: Design, Preparation, and Characterisation, *Applied Clay Science*, 246, (2023), 107180 https://doi.org/10.1016/j.clay.2023.107180

[4] Raquel Sanmartín, Vanesa Romero, Isela Lavilla, Carlos Bendicho, Ultrasound-Assisted Dispersive Micro-Solid Phase Extraction of Pb(II) in Water Samples with in Situ Synthesis of Magnetic Fe_3O_4-PbS Nanocomposites Followed by Electrothermal Atomic Absorption Spectrometry Determination, *Spectrochimica Acta Part B: Atomic Spectroscopy*, 188, (2022), 106349 https://doi.org/10.1016/j.sab.2021.106349

[5] Ellane Jacqueline Coelho Moreira Gomes, Vinicius Souza Macedo, Anna Karla dos Santos Pereira,

Grasiele Soares Cavallini, Douglas Henrique Pereira, Theoretical Study of the Adsorption Capacity of Potentially Toxic Cd^{2+}, Pb^{2+}, and Hg^{2+} Ions in Hemicellulose Matrices, *International Journal of Biological Macromolecules*, 258, (2024), 128894 https://doi.org/10.1016/j.ijbiomac.2023.128894

[6] World Health Organization, Lead Poisoning, (2025), Accessed: Nov. 02, 2025 https://www.who.int/news-room/fact-sheets/detail/lead-poisoning-and-health

[7] World Health Organization, *Guidelines for Drinking-Water Quality: Fourth Edition Incorporating the First and Second Addenda*, World Health Organization, 2022,

[8] Katayun Kiani Zadeh, Dariush Jafari, Activated carbon/alginate/Fe_3O_4 magnetic nanocomposite as a superior functional material for removal of lead from aqueous media, *Biomass Conversion and Biorefinery*, 14, (2024), 19025-19043 https://doi.org/10.1007/s13399-023-04040-z

[9] Huseyn Osman, Mehmet Uğurlu, Ali İmran Vaizoğullar, Muhammet Atasoy, Abdul Jabbar Chaudhary, Statistical modeling and optimization of heavy metals (Pb and Cd) adsorption from aqueous solution by synthesis of Fe_3O_4/SiO_2/PAM: isotherm, kinetics, and thermodynamic, *Polymer Bulletin*, 81, 16, (2024), 14513-14545 https://doi.org/10.1007/s00289-024-05404-9

[10] T. E. Oladimeji, M. Oyedemi, M. E. Emetere, O. Agboola, J. B. Adeoye, O. A. Odunlami, Review on the impact of heavy metals from industrial wastewater effluent and removal technologies, *Heliyon*, 10, 23, (2024), e40370 https://doi.org/10.1016/j.heliyon.2024.e40370

[11] Muhammad Saeed Akhtar, Sajid Ali, Wajid Zaman, Innovative Adsorbents for Pollutant Removal: Exploring the Latest Research and Applications, *Molecules*, 29, 18, (2024), 4317 https://doi.org/10.3390/molecules29184317

[12] Tahani Saad Algarni, Amal M. Al-Mohaimeed, Water purification by adsorption of pigments or pollutants via metaloxide, *Journal of King Saud University - Science*, 34, 8, (2022), 102339 https://doi.org/10.1016/j.jksus.2022.102339

[13] Muhammad Zainullah, Lya Rizka Herawati, ST. Ulfawanti Intan Subadra, Joko Utomo, Nurul Hidayat, Nur Ezaan Khamsan, Ahmad Taufiq, Synthesis and Characterization of Fe_3O_4/SiO_2/AC Nanocomposite as a Heavy Metal Adsorbent, *BIO Web of Conferences*, 2025 https://doi.org/10.1051/bioconf/202518301010

[14] Mohammed Rabeh Makhlouf, Malek Bendjaballah, Ikram Boukerche, Imane Kouadri, Sarra Hamidoud, Mohammed El Hocine Benhamza, Halim Hammi, Eco-friendly synthesis of biosorbent based in chitosan-activated carbon/zinc oxide nanoparticle beads for efficiency reduction of cadmium ions in wastewater, *Biomass Conversion and Biorefinery*, 15, 8, (2025), 12001-12016 https://doi.org/10.1007/s13399-024-05960-0

[15] Kartika Udyani, Dian Yanuarita Purwaningsih, Arlini Dyah Radityaningrum, A. Diaz, Suparto Suparto, Preparation of magnetic activated carbon based on breadfruit (*Artocarpus altilis*) peel waste by impregnation method for lead absorption in wastewater, *Ecological Engineering & Environmental Technology*, 26, 3, (2025), 95-110 https://doi.org/10.12912/27197050/199580

[16] Shadpour Mallakpour, Maryam Tukhani, Chaudhery Mustansar Hussain, Sustainable plant and microbes-mediated preparation of Fe_3O_4 nanoparticles and industrial application of its chitosan, starch, cellulose, and dextrin-based nanocomposites as catalysts, *International Journal of Biological Macromolecules*, 179, (2021), 429-447 https://doi.org/10.1016/j.ijbiomac.2021.02.183

[17] E. G. Karvelas, N. K. Lampropoulos, L. T. Benos, T. Karakasidis, I. E. Sarris, On the Magnetic Aggregation of Fe_3O_4 Nanoparticles, *Computer Methods and Programs in Biomedicine*, 198, (2021), 105778 https://doi.org/10.1016/j.cmpb.2020.105778

[18] Kyungah Seo, Kaustav Sinha, Ekaterina Novitskaya, Olivia A. Graeve, Polyvinylpyrrolidone (PVP) Effects on Iron Oxide Nanoparticle Formation, *Materials Letters*, 215, (2018), 203-206 https://doi.org/10.1016/j.matlet.2017.12.107

[19] Cristina Ileana Covaliu, Oana Stoian, Ecaterina Matei, Gigel Paraschiv, Eugenia Tanasa, Gina Alina Catrina (Traistaru), Research on Copper Ions Removal from Wastewater Using Fe_3O_4 and Fe_3O_4 Hybrid Nanomaterials, *Materiale Plastice*, 58, 1, (2021), 154-166 https://doi.org/10.37358/MP.21.1.5455

[20] Yuan Gao, Qinyan Yue, Baoyu Gao, Aimin Li, Insight into activated carbon from different kinds of chemical activating agents: A review, *Science of The Total Environment*, 746, (2020), 141094 https://doi.org/10.1016/j.scitotenv.2020.141094

[21] Phitchayaphak Saenplee, Sonchai Intachai, Panita Sumanatrakul, Panita Kongsune, Jakkree Boonlakhorn, Akkanee Pewhom, Nithima Khaorapapong, Multifunctional Magnetic Fe_3O_4@AC/NiAl-LDO Composite for Efficient Removal of Anionic and Cationic Dyes in Wastewater, *International Journal of Environmental Research*, 20, (2026), 15 https://doi.org/10.1007/s41742-025-00971-9

[22] Vo Cong Minh, Nguyen Thi Le Lien, Nguyen Thi Thuy, Le Thi Kim Phung, Nguyen Nhat Huy, Production of Biochar from Coconut Husks for Adsorption of Heavy Metals in Water, *Philippine Journal of Science*, 152, 5, (2023), 1579-1593

[23] Ahmad Taufiq, Rosy Eko Saputro, Hendra Susanto, Nurul Hidayat, Sunaryono Sunaryono, Tahta Amrillah, Husni Wahyu Wijaya, Nandang Mufti, Firman Mangasa Simanjuntak, Synthesis of Fe_3O_4/Ag nanohybrid ferrofluids and their applications as antimicrobial and antifibrotic agents, *Heliyon*, 6, 12, (2020), e05813 https://doi.org/10.1016/j.heliyon.2020.e05813

[24] Mai O. Abdelmigeed, Ahmed H. Sadek, Tamer S. Ahmed, Novel easily separable core–shell Fe_3O_4/PVP/ZIF-8 nanostructure adsorbent: optimization of phosphorus removal from Fosfomycin pharmaceutical wastewater, *RSC Advances*, 12, 20, (2022), 12823-12842 https://doi.org/10.1039/D2RA00936F

[25] Yi Fang, Lang Yang, Feng Rao, Yongming Zheng, Zhenguo Song, Adsorption behavior and mechanism of MB, Pb(II) and Cu(II) on porous geopolymers,

Ceramics International, 51, 9, (2025), 11455-11466 https://doi.org/10.1016/j.ceramint.2024.12.564

[26] Ghazal Yazdanpanah, Mohammad Reza Heidari, Najmeh Amirmahani, Alireza Nasiri, Heterogeneous Sono-Fenton like catalytic degradation of metronidazole by Fe_3O_4@HZSM-5 magnetite nanocomposite, *Heliyon*, 9, 6, (2023), e16461 https://doi.org/10.1016/j.heliyon.2023.e16461

[27] Luong Huynh Vu Thanh, Nguyen Thi Nhu Y, Nguyen Van Kiet, Ngo Truong Ngoc Mai, Nguyen Nhu Ngoc, Ly Phuong Thao, Synthesis and Application of Fe_3O_4/GO/PVP Composite Material for Methylene Blue Adsorption, *CTU Journal of Innovation and Sustainable Development*, 15, 2, (2023), 1-10 https://doi.org/10.22144/ctu.jen.2023.014

[28] Ali Ahmed Ali, Hayder M. Abdul-Hameed, Synthesis and characterization of magnetic activated carbon manufactured from palm stones by physical activation to remove lead from aqueous solution, *Desalination and Water Treatment*, 321, (2022), 100951 https://doi.org/10.1016/j.dwt.2024.100951

[29] Zahra Shahbeiki, Hojjat Nadimi, Maryam Khodadadi, Yousef Dadban Shahamat, Integrated persulfate/ozonation process using Fe_3O_4/AC catalyst for antibiotic degradation: optimization and kinetic insights, *Scientific Reports*, 16, (2026), 765 https://doi.org/10.1038/s41598-025-30357-y

[30] Md Abdus Sabur, Md Abdul Gafur, Crystallographic, Morphological, Magnetic, and Thermal Characterization of Superparamagnetic Magnetite Nanoparticles (Fe_3O_4) Synthesized by Chemical Coprecipitation Method and Calcined at 250°C for 4 hr, *Journal of Nanomaterials*, 2024, (2024), 9577778 https://doi.org/10.1155/2024/9577778

[31] Fedda Y. Alzoubi, Osama Abu Noqta, Tariq Al Zoubi, Hasan M. Al-Khateeb, Mohammed K. Alqadi, Abdulsalam Abuelsamen, Ghaseb Naser Makhadmeh, A Novel One-Pot Synthesis of PVP-Coated Iron Oxide Nanoparticles as Biocompatible Contrast Agents for Enhanced T_2-Weighted MRI, *Journal of Composites Science*, 7, 3, (2023), 131 https://doi.org/10.3390/jcs7030131

[32] Syed Afzal Zulfiqar, Rajwali Khan, Tahir Zeb, Muneeb ur Rahman, Burhanullah, Shahid Ali, Gulzar Khan, Zia ur Rahman, Akhlaq Hussain, Structural, optical, dielectric and magnetic properties of PVP coated magnetite (Fe_3O_4) nanoparticles, *Journal of Materials Science: Materials in Electronics*, 29, 23, (2018), 20040-20050 https://doi.org/10.1007/s10854-018-0134-6

[33] Samah Zaki Naji, Ching Thian Tye, Abdul Rahman Mohamed, Role of sulfuric acid modification to coconut shell activated carbon in waste cooking oil upgrading, *Biomass Conversion and Biorefinery*, 14, 5, (2024), 6967-6985 https://doi.org/10.1007/s13399-022-03018-7

[34] N. Munasir, R. Lydia, K. D. Hari, F. Nuhaa, S. S. Ezza, Synthesis of Fe_3O_4/SiO_2/PEG Nanocomposite from Minerals Sands: Kinetic Adsorption Heavy Metal Ion from Aqueous Solution, *International Journal of Engineering*, 38, 2, (2025), 330-342 https://doi.org/10.5829/ije.2025.38.02b.07

[35] Asep Bayu Dani Nandiyanto, Risti Ragadhita, Meli Fiandini, Interpretation of Fourier Transform Infrared Spectra (FTIR): A Practical Approach in the Polymer/Plastic Thermal Decomposition, *Indonesian Journal of Science and Technology*, 8, 1, (2022), 113-126 https://doi.org/10.17509/ijost.v8i1.53297

[36] Jibril Mohammed, Usman Dadum Hamza, Abdurrahman Garba, Batch and Fixed-Bed Studies of Ammonia Treated Coconut Shell Activated Carbon for Adsorption of Benzene and Toluene, *Nigerian Journal of Tropical Engineering*, 16, 1, (2022), 91-115 https://doi.org/10.59081/njte.16.1.009

[37] Nabila S. Ammar, Nady A. Fathy, Hanan S. Ibrahim, Sahar M. Mousa, Micro-mesoporous modified activated carbon from corn husks for removal of hexavalent chromium ions, *Applied Water Science*, 11, 9, (2021), 154 https://doi.org/10.1007/s13201-021-01487-1

[38] Jeffrey S. Gaffney, Nancy A. Marley, Darin E. Jones, Fourier Transform Infrared (FTIR) Spectroscopy, in: *Characterization of Materials*, Wiley, 2012, https://doi.org/10.1002/0471266965.com107.pub2

[39] Ricardo J. R. Matos, Jorge C. Silva, Paula I. P. Soares, João Paulo Borges, Polyvinylpyrrolidone Nanofibers Incorporating Mesoporous Bioactive Glass for Bone Tissue Engineering, *Biomimetics*, 8, 2, (2023), 206 https://doi.org/10.3390/biomimetics8020206

[40] Boadu Kwasi Opoku, Asiamah Isaac, Anang Akrofi Micheal, John Kwesi Bentum, Wanjala Paul Muyoma, Characterization of Chemically Activated Carbons Produced from Coconut and Palm Kernel Shells Using SEM and FTIR Analyses, *American Journal of Applied Chemistry*, 9, 3, (2021), 90 https://doi.org/10.11648/j.ajac.20210903.15

[41] Anita Yadav, Sudeep Tiwari, Vivek Kumar Salvi, Sudhish Kumar, Synthesis and characterization of sugar coated superparamagnetic $Li_{0.1}Fe_{2.9}O_4$ nanoparticles, *66th DAE Solid State Physics Symposium*, Ranchi, India, 2024 https://doi.org/10.1063/5.0177990

[42] Wenhao Yang, Wenwen Luo, Tong Sun, Yingming Xu, Yuebing Sun, Adsorption Performance of Cd(II) by Chitosan-Fe_3O_4-Modified Fish Bone Char, *International Journal of Environmental Research and Public Health*, 19, 3, (2022), 1260 https://doi.org/10.3390/ijerph19031260

[43] Md. Matiar Rahman, Abu Zar Shafiullah, Animesh Pal, Md. Amirul Islam, Israt Jahan, Bidyut Baran Saha, Study on Optimum IUPAC Adsorption Isotherm Models Employing Sensitivity of Parameters for Rigorous Adsorption System Performance Evaluation, *Energies*, 14, 22, (2021), 7478 https://doi.org/10.3390/en14227478

[44] Mahmoud F. Zawrah, Maie I. El-Gammal, Mahmoud Salem, Mervat A. El-Sonbati, Maged Ahmed, Recycling of Rice Husk for Preparation of Activated Carbon/Magnetite Nanocomposites for Removal of Methylene Blue from Wastewater, *International Journal of Environmental Research*, 17, (2023), 51 https://doi.org/10.1007/s41742-023-00542-w

[45] Sri Hastuti, Tri Martini, Atmanto Heru Wibowo, Dina Fitriana, Wihda Zuhara, Hesti Mutma'inah, Rima Indriyana Putri, Removal of Heavy Metals: Pb(II), Ni(II) and Cd(II) by $Fe_3O_4@SiO_2$-TMPDT Adsorbent Prepared from Rice Husk Ash, *ALCHEMY Jurnal Penelitian Kimia*, 21, 1, (2025), 53-63 https://doi.org/10.20961/alchemy.21.1.91934.53-63

[46] Nompumelelo Sharol Mbali Kubheka, Muthumuni Managa, Makwena Justice Moloto, Edward Ndumiso Nxumalo, Fabrication of Polyamide Thin-Film Composite/Polyethersulfone-CoreShell-Fe_3O_4/ZnO Membranes for the Efficient Removal of Pb(II) from Wastewater, *Membranes*, 15, 11, (2025), 341 https://doi.org/10.3390/membranes15110341